

Electron-impact ionization of Ar₂, ArKr, Kr₂, KrXe, and Xe₂

H. Helm*

Institut für Theoretische Physik, Universität Innsbruck, Austria

K. Stephan and T. D. Märk

Institut für Experimentalphysik, Universität Innsbruck, Austria

(Received 4 December 1978)

Relative cross sections for electron-impact ionization of the rare-gas Van der Waals dimers Ar₂, ArKr, Kr₂, KrXe, and Xe₂ have been measured with a mass spectrometer in the electron energy range from threshold to 180 eV. The following appearance potentials for direct ionization from the corresponding neutral dimers have been found: Ar₂⁺: 15.2 ± 0.2 eV, ArKr⁺: 14.0 ± 0.2 eV, Kr₂⁺: 13.45 ± 0.3 eV, KrXe⁺: 12.2 ± 0.2 eV, and Xe₂⁺: 11.75 ± 0.3 eV. These values agree with those obtained in recent photoelectron studies. The appearance potential of Ar₂⁺ formation via associative ionization of argon atoms is found to be 14.6 ± 0.2 eV.

I. INTRODUCTION

Since the pioneering work of Leckenby and Robins¹ a great many experiments with Van der Waals dimers of the rare gases have been carried out, including uv light absorption spectroscopy,² photoionization studies,³ and photoelectron spectroscopy.⁴ Studies of the electron-impact ionization function have, however, to the knowledge of the authors never been carried out. Leckenby and Robins have indeed reported an ionization efficiency curve for the process



and found it to peak strongly at around 42 eV electron energy. [Their curve is compared with our result later in this work (see Fig. 2).] These authors state, however, that their curve is falsified by instrumental effects inherent to their ion source and mass spectrometer, as the ionization efficiency curve which they obtain for the reaction



disagrees strongly with the generally accepted cross section function for process 2.

In the present work an attempt has been made to measure accurately the relative cross section functions for single ionization of various homonuclear and mixed dimers of the rare gases by electron impact. The confidence in the cross sections obtained results primarily from the success, under the same operating conditions, of the measurements of accurate cross section functions of the rare gases He, Ne, Ar, Kr, and Xe as well as the cross section ratios. The sum of the partial cross sections measured for the atomic gases was found to be in excellent agreement with the mea-

surements of the total ionization cross section by previous workers. This latter work is described in detail in a separate paper.⁵

II. EXPERIMENTAL DETAILS

Figure 1 gives a schematic drawing of the experimental apparatus used. Neutral gas under high pressure (up to 400 Torr) is stored in a thick-walled copper reservoir which may be cooled to liquid-nitrogen temperature. It then flows through a platinum nozzle *N* (diameter 0.0010 cm) into a high-vacuum region. A fraction of the emerging beam travels through a 5-mm-diam aperture *A* into the collision chamber *C*, where it is crossed at right angles by an electron beam of energy variable from 0 to 180 eV. The electron beam (1–3 μA) is guided by a weak magnetic field (about 400 G). The aperture *A* of the collision chamber lies approximately 20 mm from the nozzle *N*. At the highest inlet pressures used the background pressure in the ion source chamber reaches typically 10⁻⁵ Torr.

Ions formed in the electron beam are drawn out of the collision chamber through a slit in *L*₁ of 1.5 mm width and 8 mm height under the action of an electric field which penetrates into the collision chamber from the lens *L*₂ through the slit in *L*₁. Both *L*₁ and the pusher *P* are kept at the potential of the collision chamber *C*, which is +3 kV. The penetrating field reduces the energy of the electrons in the ionization region. From the shift in the measured appearance potential of Ar⁺ we conclude that the potential at the position of the electron beam increases nearly linearly with the potential difference *C* – *L*₂ by about 0.1/30 V. *L*₂ was typically kept at +2.7–2.8 kV. The resulting

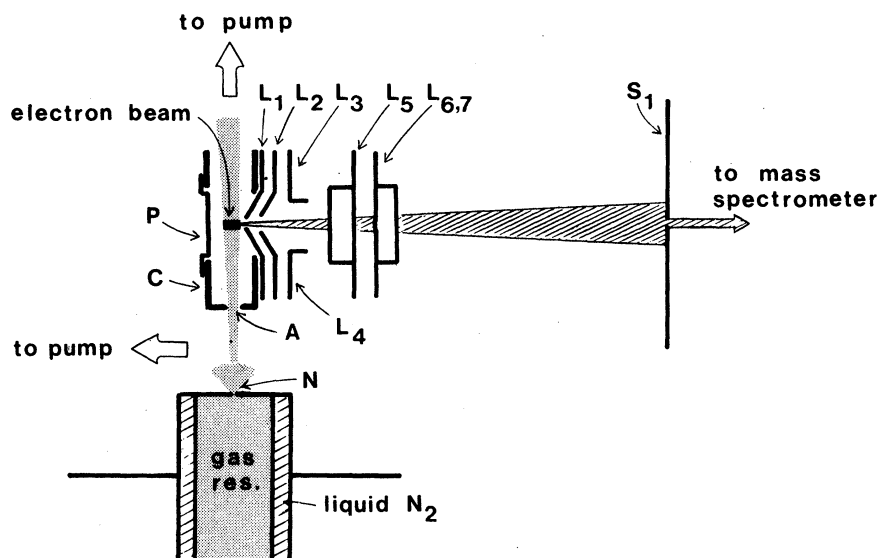


FIG. 1. Schematic drawing of gas inlet and ion source. Dimensions are approximately to scale.

penetrating field assures saturation of the ion current leaving the collision chamber, i.e., total ion collection. This saturation is observed experimentally by either measuring the total ion current in the plane of the entrance slit S_1 to the mass spectrometer or by sweeping the ion beam across the entrance slit (with deflection plates not indicated in Fig. 1) and integrating over the area of mass-analyzed ion current versus beam deflection.⁵ The ion beam at the entrance slit is several millimeters wide and only a small fraction (about 1%) may enter the mass spectrometer. The shape of the cross section curve for a given ion type could be found without sweeping the beam over the slit S_1 , provided the beam was centered approximately on the slit, within the half width of the beam. The exact position of the beam was then found not to influence the shape of the cross section curve within the reproducibility of our experiment (for dimer ions $\pm 4\%$). The mass spectrometer used is a commercial Varian MAT CH5, double-focusing mass spectrometer which has been described in detail elsewhere.⁶ The ion source, made by Varian, has been modified to the needs of the present experiments.

III. RESULTS

Molecular rare-gas ions observed with the mass spectrometer may be formed in the ion source in two ways. One is by direct ionization of the neutral dimer present in the beam leaving the reservoir (process 1). A second possibility exists via an associative ionization process⁷ (Hornbeck-Molnar process, in the following abbreviated AIP). Here a short-lived excited rare-gas atom R^* is formed

by electron impact which may subsequently combine with a neutral atom into a molecular ion by ejection of an electron



The condition is that the ionization potential of the excited atom is less than or equal to the dissociation energy of the molecular ion R_2^+ in its ground vibrational state. A detailed study of the AIP was carried out in argon in the present study in order to determine any influence of this process on the molecular ion signal and hence on the observed dimer ionization cross section. Argon was chosen since it is the rare gas which of the gases Ar, Kr, and Xe most readily undergoes reaction 3.⁷

In our apparatus Ar_2^+ could be produced via reaction 3 by using low pressures in the gas reservoir and throttling the pumping speed in the ion source chamber. The ion current of Ar_2^+ was found to increase with the square of the pressure in the ion source chamber as predicted from reaction 3; that of Ar^+ increased linearly. At a pressure of 1×10^{-4} Torr and 40-eV electron energy the molecular ion signal amounted to 0.01% of the atomic ion signal; at a pressure of 1×10^{-5} Torr to 0.001%. Figure 2(a) shows the shape of the AIP efficiency curve obtained. The curve exhibits a sharp maximum at low (~ 30 eV) electron energies, typical for the excitation process in 3. The appearance potential of Ar_2^+ from reaction 3 was found to be 14.6 ± 0.2 eV, which is in agreement with the value reported by Hornbeck and Molnar⁷ of $15.06(+0.2, -0.7)$ eV and with the value reported by Ng *et al.*³ of 14.54 ± 0.02 eV.

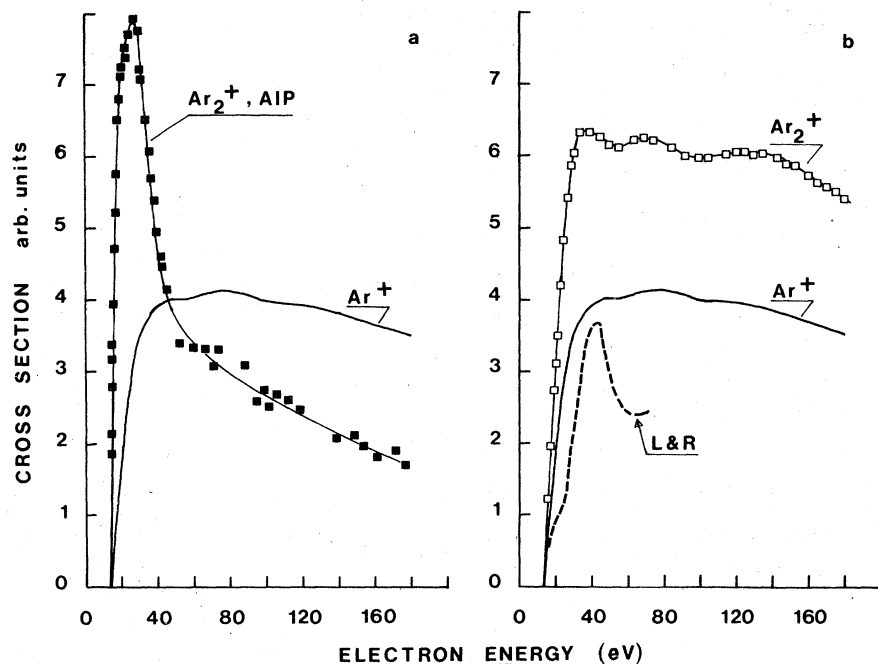


FIG. 2. Relative cross sections for electron-impact ionization of argon. Full curves (a + b): direct ionization of Ar; experimental points: (a) Ar₂⁺ production via the associative ionization process, (b) direct ionization of Ar₂ molecules; dotted curve: (b) ionization efficiency curve for Ar₂ from Ref. 1.

Reaction 3 is a disturbing factor when the ionization efficiency curve for direct ionization of the dimer is to be measured. In order to keep reaction 3 at a negligible level the gas pressure in the ionization region must be kept as low as possible, while the concentration of dimers in the beam must be made high. In argon these conditions were achieved by employing the full pumping speed in the ion source chamber and using high gas pressures in the reservoir, assisted by pre-cooling of the gas with liquid nitrogen. The dimers used in our study are either formed in the expansion process in the nozzle⁸ or are already present

in the gas reservoir due to the high gas densities.¹ We found that precooling of the gas to liquid-nitrogen temperature increased the Ar₂⁺ signal by a factor of about 100 over the signal obtained when gas at room temperature was used at the same pressure. Moreover, the dimer ion signal was found to increase with the square of the pressure in the reservoir. Typically, at a pressure of about 100 Torr and 77 K a molecular ion signal of about 0.8% of the atomic ion signal was obtained. Under these conditions the gas pressure in the ion source chamber was about 1.5×10^{-5} Torr. We therefore conclude that the contribution of the AIP

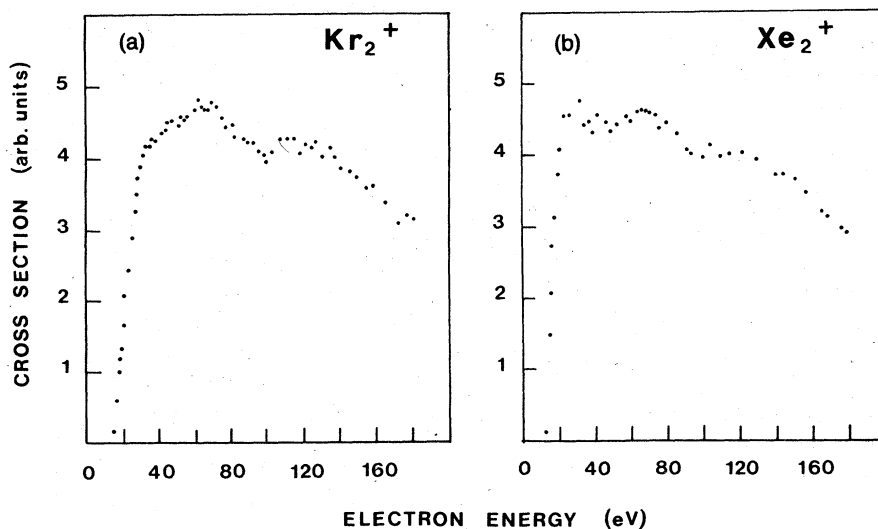


FIG. 3. (a) Relative cross section for electron-impact ionization of Kr₂; (b) relative cross section for electron-impact ionization of Xe₂.

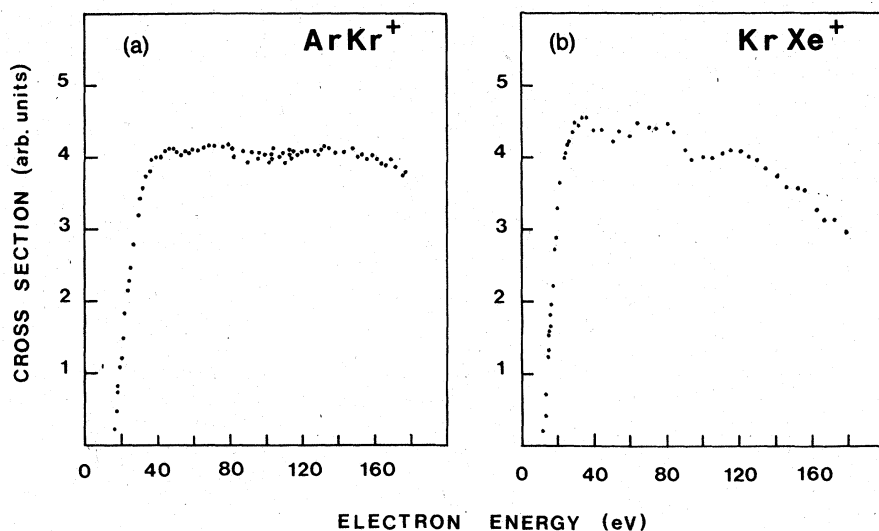


FIG. 4. (a) Relative cross section for electron-impact ionization of ArKr ; (b) relative cross section for electron impact ionization of KrXe .

to our observed molecular ion signal is less than 1%. As further evidence for this we report that the appearance potential for Ar_2^+ measured under these conditions was 15.2 ± 0.2 eV, 0.6 eV higher than the appearance potential for the AIP. The significance of this result is discussed in detail in Sec. IV. The ionization efficiency curve for Ar_2^+ produced by direct ionization of the dimer (process 1) is shown in Fig. 2(b). It is strikingly different from the observed shape of the curve to the ionization efficiency curve for atomic Ar (process 2), which is also shown in Fig. 2. It has been measured under identical conditions as the curve for ionization of Ar_2 . The shape of the ionization efficiency curve for Ar_2 which has been reported by Leckenby and Robins¹ is indicated by the dotted line in Fig. 2(b). It is significantly different from our observations.

Similar arguments concerning the contribution of the AIP to the observed molecular ion signal apply in the case of the other rare gases as well. It should be kept in mind, however, that the contribution of the AIP is still less in the other cases, since the probability of process 3 is less there⁷ and the rate of formation of neutral dimers higher in the heavier rare gases.

The mixed dimer ArKr was produced by adding about 2 Torr of krypton to 100 Torr of argon and cooling the reservoir to liquid-nitrogen temperature. For the other dimers the reservoir was operated at room temperature. For Kr_2 pressures of about 300 Torr of Kr were used. KrXe and Xe_2 were readily produced in mixtures of 20–40 Torr of xenon with 100–300 Torr of krypton. Ionization efficiency curves for direct ionization of these dimers are shown in Figs. 3 and 4. We finally report that no triatomic molecular ions and

no doubly charged molecular rare-gas ions could be detected in our experiment.⁹

IV. DISCUSSION

Figures 5–7 show our measurements of the appearance potentials for the direct ionization process of the rare-gas dimers. For comparison the measurements of the corresponding atoms are shown. The latter have been used to calibrate our electron energy scale. The resolution of our apparatus is demonstrated by the curves for Kr^+ and Xe^+ , where the change in slope due to the appearance of the metastable ions in the $^2P_{1/2}$ state is resolved. In argon no change in slope could be resolved. It may be noted that with the possible exception of KrXe^+ no changes of slope in the dimer curves are observed. One reason for this may be experimental, the lower signal-to-noise ratio in the measurements of the dimer ions.

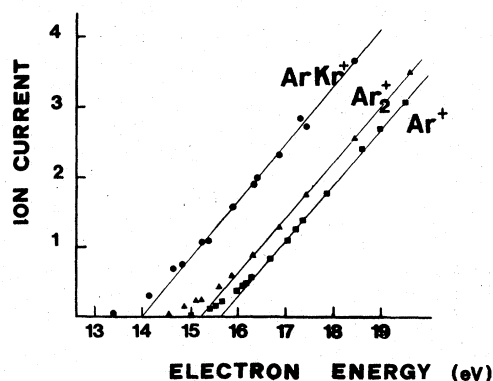


FIG. 5. Ionization efficiency curve for Ar, Ar_2 , and ArKr close to threshold.

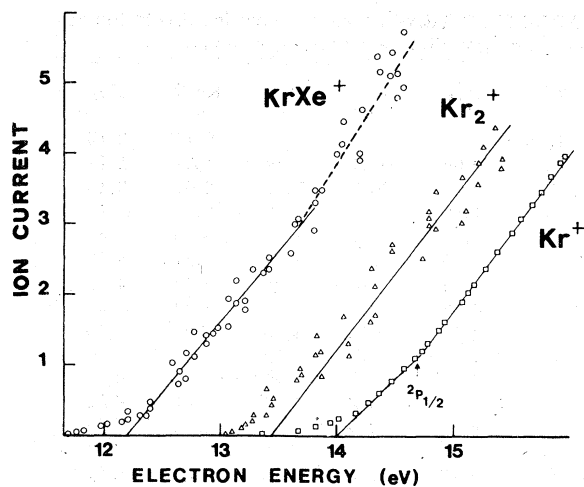


FIG. 6. Ionization efficiency curve for Kr, Kr_2 , and $KrXe$ close to threshold.

The experimentally observed appearance potentials are collected in Table I. The experimental uncertainties in the table result from the uncertainty in the energy-scale calibration via the atomic ions and the uncertainty in the extrapolation of the dimer ion signals. Our appearance potentials correspond to transitions from various vibrational levels of the neutral dimer $R_2^1\Sigma_g^+$ to the lowest R_2^+ state ($I_{\frac{1}{2}u}^+$) (see Fig. 8). The two extreme transitions from R_2 ($v=0$) and R_2 ($v=v_{max}$) are indicated in the figure. Obviously the appearance potential is influenced by the state of vibration of the dimer which is unknown in our experiment. Vertical (Frank-Condon) energy differences between R_2 and the lowest R_2^+ state may become less for higher vibrational states of R_2 , as may be seen from Fig. 8. Therefore, the theoretical values given in Table I for the vertical transition energies from R_2 ($v=0$) at the equilibrium position of the neutral dimer should represent upper limits of the appearance potentials within the accuracy

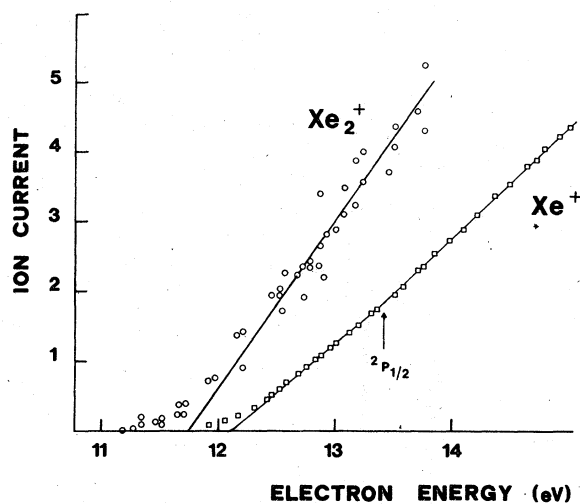


FIG. 7. Ionization efficiency curve for Xe and Xe_2 close to threshold.

of our present knowledge of the interaction potential curves. Indeed these values lie above our measured appearance potentials, though within the error limits. Directly comparable to the appearance potentials obtained in our experiment is the quantity $h\nu - E_{max}$ obtained in the measurement of the photoelectron energy distribution for the transition $R_2 - R_2^+$ ($I_{\frac{1}{2}u}^+$). Here $h\nu$ is the photon energy used in the ionization process and E_{max} the maximal photoelectron energy. Measurements of the photoelectron energy distributions have been performed recently by Dehmer and Dehmer.¹³ Values for $h\nu - E_{max}$ were obtained from Fig. 6 of Ref. 13 and are listed in Table I. Very good agreement of these data exists with the appearance potentials determined in the present work. It should be kept in mind, however, that the vibrational temperature of the dimers is likely to be lower in the Dehmer experiment, owing to vibrational cooling in the supersonic expansion process used by them; hence our energies might

TABLE I. Appearance potentials and vertical transition energies for the transition $R_2^1\Sigma_g^+ \rightarrow R_2^+I_{\frac{1}{2}u}^+$, given in eV.

Dimer	Vertical ionization energy from R_2 ($v=0$) at the equilibrium separation of R_2	Appearance potential obtained in this work	Appearance potential from high-energy limit of photoelectrons (Ref. 10)	Appearance potential obtained in photoionization study (Ref. 3)
Ar_2	15.4 ^{a,b}	15.2 ± 0.2	15.25 ± 0.05	14.54
ArKr	...	14.0 ± 0.2	...	13.43
Kr_2	13.6 ^{a,c}	13.45 ± 0.3	13.55 ± 0.05	12.86
KrXe	...	12.2 ± 0.2	...	11.76
Xe_2	11.9 ^{a,d}	11.75 ± 0.3	11.70 ± 0.05	11.10

^aUsing equilibrium separation values given in Ref. 2.

^bUsing the R_2^+ potential of Ref. 10.

^cUsing the R_2^+ potential of Ref. 11.

^dUsing the R_2^+ potential of Ref. 12.

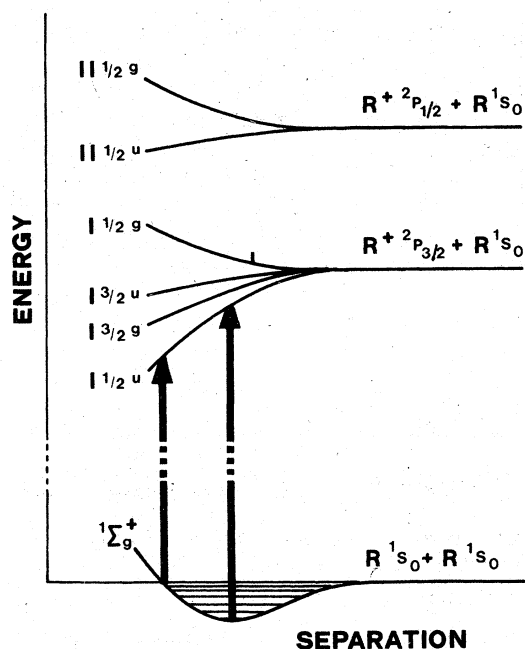


FIG. 8. Schematic potential-energy diagram versus internuclear separation regarding the direct ionization of homonuclear rare-gas dimers. Only the transitions to the lowest R_2^+ state are indicated.

lie somewhat lower than those obtained in Ref. 13. This effect, however, appears to be within the uncertainty of our measured values.

Finally, the appearance potentials for photoionization of rare-gas dimers determined by Ng *et al.*³ are quoted in Table I. These appearance potentials are determined from the onset of the molecular ion current as the photon energy increases. The appearance potentials determined by Ng *et al.* all lie approximately 0.6 eV lower than the values obtained in our electron-impact ionization experiment, and thus seem to correspond to an excitation process of one atom in the dimer, followed by autoionization of the $R-R^*$ complex. This process is basically equivalent to process 3. Hence the value which was obtained in Ref. 3 for the onset of Ar_2^+ (14.54 ± 0.02 eV) should be directly comparable to the appearance potential which we measured for reaction 3 in Ar (14.6 ± 0.2 eV) if the binding energy of the Ar_2 (ν) molecule (<0.01 eV) is added to our value. The agreement is satisfactory, as noted in Sec. III.

Owing to the lack of sensitivity and resolution in our experiment we were unable to detect a contribution due to autoionization of the neutral dimers below the threshold of direct ionization. The low-energy tail of our appearance potential curves is smeared out owing to the width of the energy distribution of our ionizing electrons, for which we measured a full width at half-maximum of about

TABLE II. Relative cross sections for direct ionization of rare-gas dimers by electron impact.

(eV)	Ar_2	ArKr	Kr_2	KrXe	Xe_2
12.5				0.15	0.15
15	0.04	0.24	0.44	1.09	1.78
17.5	0.76	0.83	1.11	2.07	3.10
20	1.82	1.44	1.89	2.88	3.75
25	3.25	2.57	3.07	4.10	4.58
30	3.87	3.47	4.04	4.41	4.70
35	4.15	3.86	4.24	4.54	4.52
40	4.22	4.02	4.37	4.39	4.44
45	4.19	4.14	4.55	4.35	4.54
50	4.12	4.07	4.52	4.23	4.39
55	4.13	4.09	4.59	4.34	4.48
60	4.16	4.12	4.77	4.32	4.54
70	4.18	4.19	4.76	4.38	4.63
80	4.12	4.12	4.47	4.46	4.44
90	4.06	4.03	4.21	4.08	4.18
100	4.00	4.00	4.00	4.00	4.00
110	4.03	3.93	4.24	4.03	4.01
120	4.05	4.11	4.19	4.08	4.05
130	4.05	4.13	4.01	3.94	3.98
140	4.01	4.09	3.84	3.77	3.72
150	3.96	4.03	3.68	3.58	3.70
160	3.87	4.02	3.50	3.41	3.35
170	3.78	3.94	3.17	3.15	3.12
180	3.69	3.75	3.09	2.90	2.86

0.25 eV.

The absolute values of the cross sections of the rare-gas dimers are of practical interest, as these might be used to determine the concentration of dimers present in atomic beams. An absolute calibration by the molecular flow technique as it is used for conventional gases⁶ is currently considered too inaccurate, as it would involve a theoretical estimate of the concentration of dimers in the reservoir as well as the assumption of no loss and no additional production of dimers in the effusion process. We therefore suggest the use of the simple qualitative rule¹⁴ that the cross section for diatomic molecules is the sum of the cross sections of the individual partners. It must be kept in mind here, however, that of the six potential-energy curves of the homonuclear ions R_2^+ (see Fig. 8) which may be reached in the direct ionization process, two are repulsive in the separation regime of interest here. Ions formed in these by vertical transitions will dissociate and therefore not contribute to the measured molecular ion signal. To account for this the factor 2 should be replaced by a factor $\frac{4}{3}$, which also takes into account the statistical weighting of the various states. For the mixed molecular ions interaction potentials are currently not available. Our measured relative cross sections have been arbitrarily normalized to a value of 4 at 100 eV electron energy, and are given in Table II as a function of electron energy.

V. CONCLUSIONS

The relative cross section functions for electron-impact ionization of various Van der Waals dimers of the rare gases are found to be similar to those for the corresponding rare-gas atoms. This is in strong contrast to the observations reported by Lee and Fenn,¹⁵ who studied the ratio of dimer to monomer ion current with a quadrupole mass spectrometer at 48 and 60 eV electron energy. They find in argon that increasing the electron energy from 48 to 60 eV the ratio of dimer ion current to monomer ion current decreases by a factor 2. Our measurements in argon indicate, however, that the cross section ratio for dimers to monomers is *constant* for electron energies above 40 eV within $\pm 4\%$ [see Fig. 2(b)]. We argue that the observations made by Lee and Fenn¹⁵ reflect intrinsic problems with their extraction system. Uncontrolled extraction and focusing conditions in an ion source may produce large errors in the shape of ionization efficiency curves, as has been demonstrated recently.^{16,17}

Our measured cross section functions for ionization of the dimers show no similarity with the cross section curve for associative ionization of rare-gas atoms. This latter process would be

equivalent to an autoionization process in the dimer. The appearance potentials and the cross section functions found indicate that the direct ionization of the rare-gas dimers dominates the ionization event. The appearance potentials found in the present study are in agreement with results from photoelectron energy measurements.¹³ They are also consistent with theoretical predictions based on the interaction potential curves for the Van der Waals dimers and the molecular rare-gas ions.

ACKNOWLEDGMENTS

The authors are grateful to the Österreichischer Fonds zur Förderung der Wissenschaftlichen Forschung for financial assistance under projects No. 1490, 1727, and 2781. The authors wish to thank Professor M. Pahl for the opportunity to use the mass spectrometer system CH 5, and would like to acknowledge helpful cooperation in the early stage of this study from Professor A. Rutscher, Sektion Physik/Elektronik, Universität Greifswald. We are grateful for a critical reading of the manuscript by Professor R. N. Varney, guest professor at the Institut für Atomphysik, Universität Innsbruck.

*Current address: Molecular Physics Center, SRI International, Menlo Park, Calif. 94025.

¹R. E. Leckenby and E. J. Robins, Proc. R. Soc. Lond. Sect. A **291**, 389 (1966).

²D. E. Freeman, K. Yoshino, and Y. Tanaka, J. Chem. Phys. **67**, 3462 (1977).

³C. Y. Ng, D. J. Trevor, D. H. Mahan, and Y. T. Lee, J. Chem. Phys. **66**, 446 (1977); C. Y. Ng, P. W. Tiedemann, B. H. Mahan, and Y. T. Lee, J. Chem. Phys. **66**, 5737 (1977).

⁴P. M. Dehmer and J. L. Dehmer, J. Chem. Phys. **68**, 3462 (1978).

⁵K. Stephan, H. Helm, and T. D. Märk (unpublished); in *Proceedings of the Symposium on the Physics of Ionized Gases, Dubrovnik, 1978*, of Abstracts, p. 77.

⁶T. D. Märk and F. Egger, Int. J. Mass Spectrom. Ion Phys. **20**, 89 (1976).

⁷J. A. Hornbeck and J. P. Molnar, Phys. Rev. **84**, 621 (1951).

⁸T. A. Milne and F. T. Greene, J. Chem. Phys. **47**, 4095 (1967).

⁹The detection limit for trimer ions is approximately 1% of that of the singly charged dimer ions, for the

doubly charged dimer ions approximately 5% of that of the singly charged dimer ions.

¹⁰J. T. Moseley, R. P. Saxon, B. A. Huber, P. C. Cosby, R. Abouaf, and M. Tadjeddine, J. Chem. Phys. **67**, 1659 (1959).

¹¹R. Abouaf, B. A. Huber, P. C. Cosby, R. P. Saxon, and J. T. Moseley, J. Chem. Phys. **68**, 2406 (1978).

¹²W. R. Wadt, D. C. Cartwright, and J. S. Cohen, Appl. Phys. Lett. **31**, 672 (1977).

¹³P. M. Dehmer and J. L. Dehmer, J. Chem. Phys. **69**, 125 (1978).

¹⁴J. W. Otvos and D. P. Stevenson, J. Am. Chem. Soc. **78**, 546 (1956).

¹⁵N. Lee and J. B. Fenn, Rev. Sci. Instrum. **49**, 1269 (1978).

¹⁶T. D. Märk, F. Egger, E. Hille, M. Cheret, H. Störi, and K. Stephan, in *Proceedings of the Tenth International Conference on the Physics of Electronic and Atomic Collisions, Paris, 1977* (Commissariat a l'Energie Atomique, Paris, 1977), p. 1070.

¹⁷E. Hille, T. D. Märk, and H. Störi, in *Proceedings of the First Symposium on Atomic and Surface Physics, Tirol, 1978* (Lindiguer, Innsbruck, 1978), p. 59.